DOI: 10.1002/adma.200701681

Electrostatic Properties of Ideal and Non-ideal Polar Organic Monolayers: Implications for Electronic Devices**

By *Amir Natan*, *Leeor Kronik*,* *Hossam Haick*, and *Raymond T. Tung*

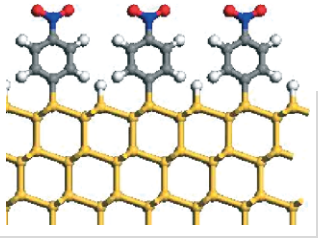

Molecules in (or as) electronic devices are attractive because the variety and flexibility inherent in organic chemistry can be harnessed towards a systematic design of electrical properties. Specifically, monolayers of polar molecules introduce a net dipole, which controls surface and interface barriers and enables chemical sensing via dipole modification. Due to the long range of electrostatic phenomena, polar monolayer properties are determined not only by the type of molecules and/or bonding configuration to the substrate, but also by size, (dis-)order, and adsorption patterns within the monolayer. Thus, a comprehensive understanding of polar monolayer characteristics and their influence on electronic devices requires an approach that transcends typical chemical designs, i.e., one that incorporates long-range effects, in addition to short-range effects due to local chemistry. We review and explain the main uses of polar organic monolayers in shaping electronic device properties, with an emphasis on long-range cooperative effects and on the differences between electrical properties of uniform and non-uniform monolayers.

[*] Dr. L. Kronik, A. Natan
Department of Materials and Interfaces
Weizmann Institute of Science
Rehovoth 76100 (Israel)
E-mail: leeor.kronik@weizmann.ac.il
Dr. H. Haick
Department of Chemical Engineering and
Russell Berrie Nanotechnology Institute
Technion – Israel Institute of Technology
Haifa 32000 (Israel)
Prof. R. T. Tung
Department of Physics
Brooklyn College of the City University of New York
Brooklyn, NY 11210 (USA)

[**] We thank Ron Naaman (Weizmann Institute), David Cahen (Weizmann Institute), Dudi Deutsch (Weizmann Institute), and Abraham Nitzan (Tel Aviv University) for many illuminating discussions. Work in Rehovoth was supported by the "Bikura" track of the Israel Science Foundation, the Gerhard Schmidt Minerva Center for Supra-Molecular Architecture, and the historic generosity of the Harold Perlman family. LK holds the Delta Career Development Chair and is an *ad personem* member of the Lise Meitner Center for Computational Chemistry. HH holds the Horev Chair for Leaders in Science and Technology and acknowledges a Marie Curie Excellence Grant of the EC's FP6 and the Russell Berrie Nanotechnology Institute for support. RTT gratefully acknowledges financial support from the National Science Foundation (DMR-0706138). HH and RTT also thank the US-Israel Binational Science Foundation for financial support.

1. Introduction

Molecular electronics, which involves the use of molecules and molecular assemblies as passive and active electronic devices,[1–3] has attracted much attention because it allows for the design and realization of novel nano-scale devices. A related, but conceptually different, approach is to use molecular functionality to influence and control the characteristics of otherwise conventional electronic devices.[4,5] In this way, one can benefit from both the inherent design flexibility offered by molecules and the maturity and robustness of semiconductor-based electronic devices, so as to enjoy the best of both worlds. For example, hybrid structures comprised of molecular layers adsorbed on semiconducting or metallic substrates have been shown to exhibit novel electro-optical[6,7] and magnetic[8,9] properties that the individual components do not necessarily possess on their own.

Here, we focus on one specific strategy for modifying electronic device properties with molecules, viz. use of *polar* monolayers at surfaces and interfaces.[4,5,10] Generally, a polar monolayer introduces a net electrical dipole perpendicular to the surface/interface.[10] This results in a potential shift that modifies the work function and electron affinity at a surface

ADVANCED MATERIALS

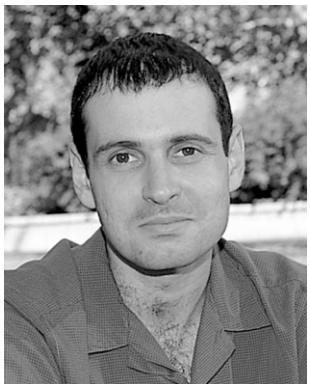

Dr. Leeor Kronik is a Senior Scientist with the Department of Materials and Interfaces at the Weizmann Institute of Science, Israel. His current research interests focus on understanding and predicting electronic, optical, and magnetic properties of materials from first principles. Emphasis is currently placed on nano-materials, spintronic materials, and organic electronic materials, as well as on methodological advances within density functional theory. He obtained a Ph.D. in physical electronics from Tel-Aviv University, Israel. He pursued post-doctoral studies as a Fulbright scholar with the Department of Chemical Engineering and Materials Science at the University of Minnesota and as a research fellow with the Minnesota Supercomputing Institute. He is a recipient of the 2006 Young Investigator Krill prize of the Wolf Foundation for excellence in scientific research and a member ad personem of the Lise Meitner-Minerva Center for Computational Quantum Chemistry.

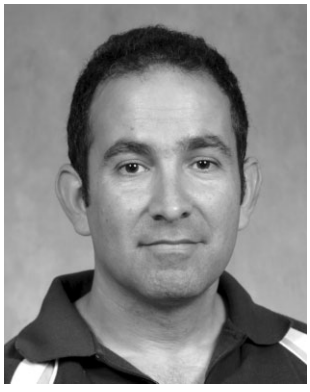

Amir Natan received his B.Sc. in Physics and Mathematics from the Hebrew University (1987) and his M.Sc. In Electrical Engineering from Tel-Aviv University (2005). He is currently a Ph.D. student at the Weizmann Institute of Science at the faculty of Chemistry. He has worked in industry in the fields of signal processing, radar detection, and bioinformatics. He is a co-founder of Compugen Ltd., a leading company in the development of algorithms for research of the human genome.

Dr. Hossam Haick has been a faculty at the Department of Chemical Engineering and Russell Berrie Nanotechnology Institute of the Technion since 2006. He received his B.Sc. and Ph.D. in Chemical Engineering from the Ben-Gurion University (1998) and Technion – Israel Institute of Technology (2002), respectively. After a two-year period at the Weizmann Institute of Science (2002-2004), he moved to the California Institute of Technology – Caltech (2004–2006) for a postdoctoral research. Among his honors are the Horev Chair for Leaders in Science and Technology, the Marie Curie Excellence Award, the Bergmann Award, the Minerva Award, and the Kahannof award for excellent young scientists. The research interests of Dr. Haick include electronic nose devices, nanomaterials-based chemical sensors, molecule-based electronic devices, electrical contacts to molecules, electronic charge transport through organic molecules and molecularly-modified metal/semiconductor junctions.

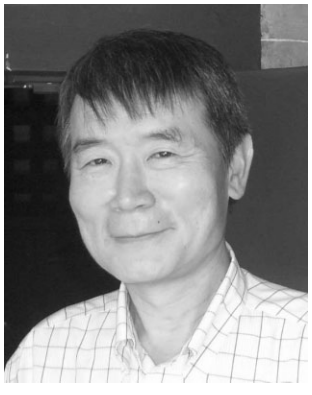

After Raymond Tung received his Ph.D. in physics from the University of Pennsylvania, he joined Bell Labs's basic research staff and worked in the general area of electronic materials and interfaces. Most notably, he has worked on the epitaxial growth of metallic thin films, the formation mechanism of Schottky barrier heights, silicide formation, and shallow junction. In 2002, he joined the faculty of Brooklyn College, City University of New York, where he is now a professor and acting chair of the physics department. In 1996 and 2001–02, he occupied the visiting chair position at the Research Center for Quantum Effect Electronics of the Tokyo Institute of Technology.

and changes the band offset and band bending at an interface. This dipole effect is a general one and can be obtained with non-molecular treatments as well.[11–13] Nevertheless, the use of molecules, especially organic ones, allows a systematic tuning of the desired dipole moment by an appropriate choice of the functional group.[4] Because several functional groups can be attached to the same basic unit, optimal dipole design can be achieved together with optimal design of other pertinent chemical and (opto)-electrical properties, e.g., binding group(s), frontier orbital energy levels, etc.[14]

The dipole associated with a polar monolayer is usually modeled within the semi-classical Helmholtz picture, which effectively treats the monolayer as a dielectric "parallel plate capacitor".[10,15] Predictions from this simple picture often provides qualitative or semi-quantitative understanding of results from polar molecular layers at surfaces and interfaces. However, significant difficulties in data interpretation within this simple picture have also been encountered. One example is the demonstrated modulation of current in the channel of a field effect transistor (FET) upon adsorption of a polar layer, where the molecular dipole substitutes or augments the transistor's gate.[16–18] As there is no electric field outside a dipole layer in the parallel plate capacitor model, it is difficult to understand why this device actually works experimentally.[17] Another example is that changes observed in the current-voltage behavior of Schottky diodes possessing a polar monolayer at the metal/semiconductor interfaces are inconsistent with the Helmholtz dipole at the interface.[19]

Obviously, a molecular layer is different from a textbook parallel plate capacitor. On the scale of inter-atomic distances, even a perfectly ordered layer of molecules is a quantum mechanical object with rapid variations in charge density along both the lateral and the vertical directions. Up close, the electric field distribution of a molecular layer is quite different from that of a classical parallel plate capacitor with its charge assumed to be perfectly smeared out in the lateral directions. These marked differences immediately raise two questions: First, do the problems associated with the above-described experimental observations suggest that a more realistic view of ideal monolayers needs to be adopted, or are they a manifestation of significant deviations from monolayer ideality (via, e.g., pinholes, domains, periodic patterns, disorder, etc.)? Second, to what extent can we still rationalize the experimental results semi-classically, albeit with a refined model, and where, if at all, are we observing inherently quantum effects?

To answer these questions, we offer here a comprehensive analysis of the electrostatics of polar monolayers, where each molecule is modeled as a classical point dipole. In Section 2, we use this model to analyze *ideal* (i.e., perfectly periodic) monolayers. We compare and contrast the predictions of this simple approach with first principles quantum mechanical calculations using density functional theory (DFT), reported in the literature for a variety of substrates and polar adsorbates. We then show that the point dipole model not only captures the main features of the computational studies but also provides an underlying rationale for the successes of the parallel plate capacitor picture for certain experimental findings. In Section 3, we use the point-dipole model to examine how the electrostatic properties of *non-ideal* monolayers differ from those of the ideal ones. We show how non-ideality can explain experimental results that are unexplained by the Helmholtz picture and provide guidelines for the prediction of new experimental results. Additionally, we examine how the picture is modified for polar molecule adsorption on lower-dimensional structures, especially 1d nano-wires. Finally, a summary and outlook is given in Section 4.

2. Electrostatics of Ideal Polar Monolayers

We define an ideal molecular monolayer as an infinite, defect-free, two-dimensional periodic array of molecules. An overview of its electrostatics is a natural starting point for our analysis. First, this system is "closest in spirit" to the ideal parallel plate capacitor, an issue elaborated below. Second, first principles calculations with a manageable unit cell size can be performed readily for ideal monolayers, because of the cell periodicity.[20] Comparing the simple electrostatics analysis to full-fledged quantum mechanical calculations can, thus, serve to examine its validity and to understand its limitations. As the simplest possible representation for an ideal monolayer beyond the parallel plate capacitor model, we consider a periodic array of point dipoles with the inter-molecular spacing. This effectively ignores all quantum mechanical aspects of the molecular assembly, e.g., any details of chemical bonds with the substrate.

The potential and field at a point $\vec{r}$ due to a point dipole $\vec{p}$ at the origin is given (in cgs units) by[21]

$$V = \frac{\vec{p}\cdot\vec{r}}{r^3};\ \vec{E} = \frac{1}{r^3}[3(\vec{p}\cdot\hat{r})\hat{r} - \vec{p}] \tag{1}$$

where $r = |\vec{r}|$ and $\hat{r} = \vec{r}/r$. For simplicity, we assume that the dipole is pointing in the z direction. In this case, the potential and electric field simplify to

$$V(\vec{r}) = p\cos\theta/r^2;\ E_r(\vec{r}) = 2p\cos\theta/r^3;\ E_\theta(\vec{r}) = p\sin\theta/r^3 \tag{2}$$

where V is the potential, E_r and E_θ are the electric field components in the direction of $\vec{r}$ and perpendicular to that direction, respectively, and θ is the polar angle.

When an array of dipoles is assembled, the potential and electric field simply add up according to the superposition principle. However, it is important to remember that molecules are *polarizable* and, therefore, their net dipole moment may change in response to external electric fields, such as those due to dipoles of other molecules. A simple electrostatic model of this phenomenon was constructed by MacDonald and Barlow.[22] They showed that, to first order, molecular po-

ADVANCED MATERIALS

larizability can be taken into account by relating the molecular dipole p to the gas phase molecular dipole p_0 via

$$p = p_0 + aE_z \tag{3}$$

where E_z is the external electric field at the position of the point dipole and a is the molecular polarizability. For each point dipole, a summation over the electric field due to the infinite 2d array of all other dipoles shows that the net external electric field it feels is[23]

$$E_z = -\frac{kp}{a^3} \tag{4}$$

where a is the inter-dipole distance along one direction of periodicity and k is a constant – first computed by Topping[23] – that depends only on the geometry of the periodic array. For example, $k \cong 9.034$ for a square unit cell and $k \cong 11.034$ for a triangular unit cell. Combining Equations 3 and 4 yields[22]

$$p = \frac{p_0}{1 + ak/a^3} \tag{5}$$

Equation 5 reveals that a *depolarization*, i.e., a reduction of the molecular dipole with respect to its gas phase value, is expected. Physically, each molecule experiences an electric field due to all other molecules, which points in a direction opposite to that of the molecule's own dipole. Therefore, the molecule partially depolarizes in response to this on-site electric field. This tendency can also be understood in terms of the Le Chatelier principle: as the molecules are brought closer together, the electrostatic energy of the system increases. The molecular depolarization reduces this increase and therefore acts so as to counteract the perturbation.[24]

The depolarization phenomenon predicted by Equation 5 has been found in many experimental studies of the dipole of polar monolayers (cf., e.g., ref. [24]). In most cases the findings were interpreted using an empirical dielectric constant, the relation of which to the polarizability picture presented here is discussed below. However, an *explicit* and elegant use of Equation 5 for interpreting experimental data has been given recently by Fukagawa et al.[25] They measured work function changes upon adsorption of titanyl phthalocyanine (OTiPc) on graphite, as a function of coverage, as shown in Figure 1a. By computing the dipole density from the coverage and using this value in Equation 5, they were able to obtain a very good fit with the experimental data and to deduce an experimental value for the molecular polarizability.

Recently, Equation 5 has also been used successfully for interpreting quantum mechanical calculations of potential and dipole trends in polar monolayers.[26–29] Importantly, these studies analyzed very different substrates, molecules, and bonding configurations. The fact that the simple electrostatic model embodied in Equation 5 was found to be useful in all of these cases strongly suggests that the pertinent phenomenology is indeed governed by classical, rather than quantum, effects. As an example, a comparison of the predictions of Equation 5 with DFT calculations for a series of benzene derivatives adsorbed on the Si(111) surface is shown in Fig-

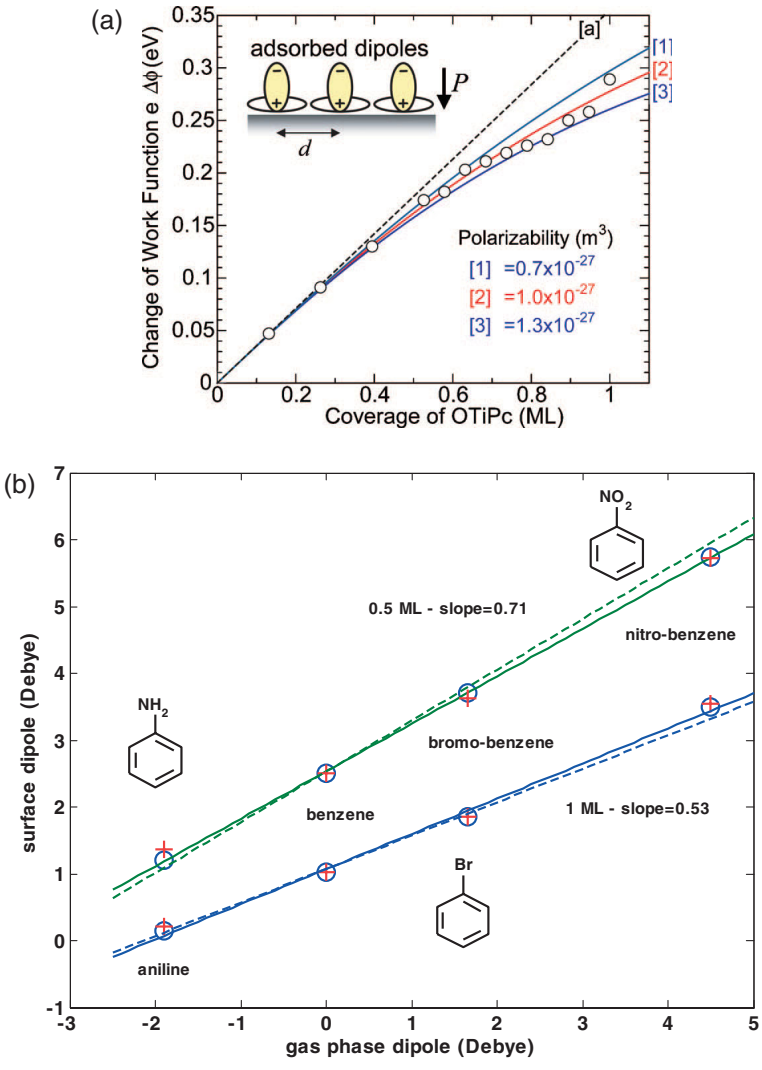

Figure 1. a) Circles: Experimental dependence of the work function of a graphite substrate on OTiPc coverage. The dashed line represents the limiting behavior in the low coverage region (~ 0.3 monolayer). Curves 1–3 represent fitting with different polarizability values using Equation 5. Inset: A schematic representation of the molecular orientation and direction of the dipoles in the monolayer. Reproduced from [25], with permission, copyright 2006 American Institute of Physics b) DFT-computed surface dipole (to within an arbitrary constant), in Debye units (1 Debye $\cong 3.3 \times 10^{-30}$ Cb·m) as a function of gas phase dipole for different benzene derivatives adsorbed on a Si(111) substrate and for both 1 monolayer and 0.5 monolayer coverage. Circles: DFT-computed values. Crosses: computed values upon removal of the Si substrate, i.e., for a "free standing" molecular film. Solid lines: linear fit of the DFT results. Dashed lines: results obtained from Equation 5 using the known polarizability of benzene. All DFT data used were taken from [26], with permission.

ure 1b.[26] The agreement between the classical and quantum calculation is very good and is particularly remarkable, given that the lateral distance between the molecules is similar to their length, i.e., point dipole is not a good approximation for these molecules. Note, however, that Equation 5 only addresses the dielectric response of *individual* molecules. In densely packed molecular layers, collective effects due to inter-molecular[30] or molecule-substrate[31] interactions, as well as significant structural changes,[32] may take place so as to further depolarize the monolayer.

Having understood how each molecular dipole is affected by the presence of other dipoles, the remaining major question is what electrical potential is generated by an *array* of (possibly partially depolarized) dipoles. To answer this question we consider an infinitely periodic array of finite-length dipoles, i.e., an infinitely periodic sheet of negative point charges at the $z = 0$ plane, separated from an infinitely periodic sheet of positive point charges at the $z = d$ plane. For simplicity (and with no loss of generality for the physical conclusions given below), we assume a rectangular unit cell with rectangle sides of dimensions a and b. The overall spatial charge distribution, $\rho(x, y, z)$, is then given by:

$$\rho(x,y,z) = q\left(\sum_{k,l=-\infty}^{\infty}\delta(x-ka,y-lb,z-d)-\sum_{k,l=-\infty}^{\infty}\delta(x-ka,y-lb,z)\right) \quad (6)$$

where q is the proton charge and $\delta(\cdot)$ is the Dirac delta function. This charge distribution results in a periodic potential. Its form outside the dipolar double layer can be expressed as a Fourier series as an immediate consequence of the expansion given by Lennard-Jones and Dent for a planar periodic array of monopoles.[33] The result is[34]

$$V(x,y,z) = V_{av} + {\sum_{m,n=-\infty}^{\infty}}' \frac{q}{ab\sqrt{(m/a)^2+(n/b)^2}} e^{i2\pi\left(\frac{mx}{a}+\frac{ny}{b}\right)} \left[e^{-2\pi\sqrt{(m/a)^2+(n/b)^2}|z-d|} - e^{-2\pi\sqrt{(m/a)^2+(n/b)^2}|z|}\right] \quad (7)$$

where

$$V_{av}(z>0) - V_{az}(z<0) = \frac{4\pi qd}{ab} \quad (8)$$

and the prime in the summation indicates exclusion of the m=n=0 term. Furthermore, if we let $d \to 0$ while keeping the dipole p=qd constant, we obtain[35]

$$V(x,y,z) = V_{av} + {\sum_{m,n=-\infty}^{\infty}}' \frac{2\pi p}{ab} e^{i2\pi\left(\frac{mx}{a}+\frac{ny}{b}\right)} e^{-2\pi\sqrt{(m/a)^2+(n/b)^2}|z|} \quad (9)$$

The salient point of Equations 7–9 is that for an infinite, periodic 2d array of dipoles, the power-law behavior of an isolated dipole (Eq. 1) is replaced by a sum of exponentially decaying terms. The decay is slowest for $m = 1$, $n = 0$, or $m = 0$, $n = 1$, i.e., the maximal decay length is $l_{\max} = \max(a/2\pi, b/2\pi)$. This means that, for either a point dipole (Eq. 9) or a finite dipole (Eq. 7), outside the dipolar sheet the potential rapidly converges to a constant because of the rapidly decaying exponential terms. We note that the striking differences in the behavior of an ensemble of identical objects from that of a single one are well-known in electromagnetic theory, e.g., in the analysis of antenna arrays.[36] Such differences are equally valid for nano-scale objects because the laws of electrostatics are scale independent.

An illustration of this effect is given in Figure 2, where the magnitude of the electrostatic field due to an isolated dipole and a planar dipolar array are compared. It is readily observed that the electric field decrease is indeed much more pronounced for the dipolar layer than for the isolated dipole. Importantly, there exists a significant range of z values where the single dipole field is significant but the monolayer field is already negligible. This range of z values is *inherently* of the order of lateral dipole distances, as the vertical decay length, $l_{\max}$, is proportional to (and smaller by 2π than) the maximal lateral inter-molecular distance.

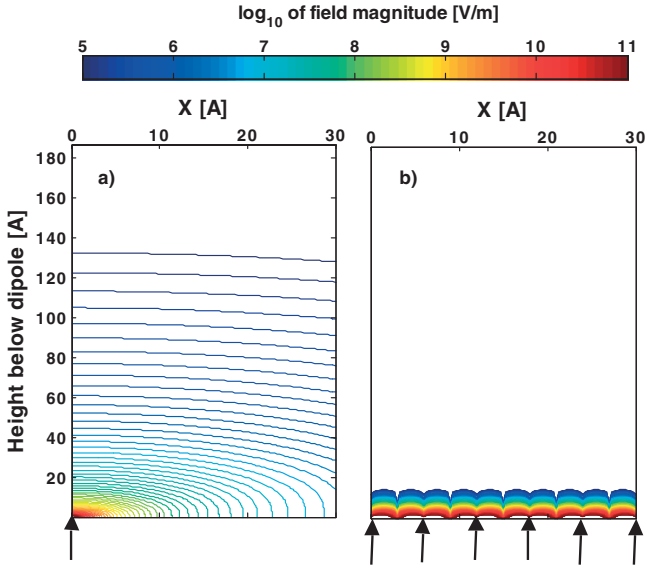

Figure 2. Distribution of the electric field magnitude, on a logarithmic scale, in the *xz* plane due to: a) A single dipole with $p = 4$ Debye and $d = 2$ Å; b) A square array of such dipoles with inter-dipole separation of $a = b = 6$ Å. Dipole positions are indicated on the figure as arrows.

Physically, the difference between a single point dipole and a sheet of point dipoles can be further understood by considering that the electric field lines of a point dipole must form closed loops. At any given point slightly below the xy plane, the z-component of the electric field due to dipoles positioned directly above this point (i.e., those positioned near $(x,y,0)$) is of opposite sign to that from dipoles that are laterally far from

ADVANCED MATERIALS

this point. The lateral components of the electric field also tend to cancel. For example, the y-component of the electric field due to dipoles positioned at the half-plane (x',$y' > y$,0) is of opposite sign to that due to dipoles positioned at the other half (x',$y' < y$,0). At a point close to the xy plane, the extent of the "left-right" and "near-far" cancellations depends on the exact lateral location (x,y) of this point relative to the mesh of the molecular dipoles. As one moves away from the dipolar layer, things smooth out, the electric field becomes increasingly negligible, and the potential becomes increasingly close to a constant.

Again, it is appropriate to ask whether the electrostatics predictions can really explain first principles quantum mechanical calculations. First, the basic phenomenology of Figure 2, namely, the induction of significant electric fields in an underlying substrate from a single polar molecule, but not from a molecular monolayer, *despite the same local chemistry in both cases* (i.e., the same molecule being bound to the same substrate in the same way), has been recently confirmed by the detailed DFT calculations of Deutsch et al.[37] Furthermore, we argue that the suppression of significant electric fields in the substrates explains systematically a host of recent monolayer results that may appear puzzling from a traditional chemical point of view.

Consider again the results of Figure 1b. Remarkably, the figure also shows that the relative difference in the surface dipoles due to different benzene derivatives is almost completely independent of whether the Si substrate is present or absent in the calculation. Natan et al. have argued that this is an immediate consequence of the rapid decay of the electric field outside the polar group.[26] This argument is confirmed explicitly in Figure 3a, where the average electrostatic potential along the z-axis is shown for several of the Si(111)-adsorbed benzene derivatives of Figure 1b. Clearly, the potential differences resulting from a change of the polar group decay rapidly away from the position of the polar group. These differences become insignificant by the middle of the benzene ring and are completely negligible at the position of the Si substrate. These arguments also explain the recent DFT results of Heimel et al.,[29,40,41] shown in Figure 3b, where a change of the polar group for Au(111)-adsorbed conjugated thiols yielded only an additive change of surface work function, i.e., there was no significant interaction of the dipole field with the substrate. Again, this is clearly a consequence of the fact that the electrostatic potential induced by the polar group decays rapidly through the farther aromatic ring and can no longer be "felt" by the Au substrate.

Generally speaking, one can predict from similar arguments that when both the head and tail group of a sufficiently long molecule are polar, the overall monolayer dipole will be close to a simple sum of the two dipoles, because of the negligible extent of the field due to one dipolar sheet at the position of the other. Interestingly, this additivity has been noted as a curious experimental observation already in the 1930s, for a film of dibasic esters on water.[42] In more modern times, a similar additivity between the dipole due to the functional group and

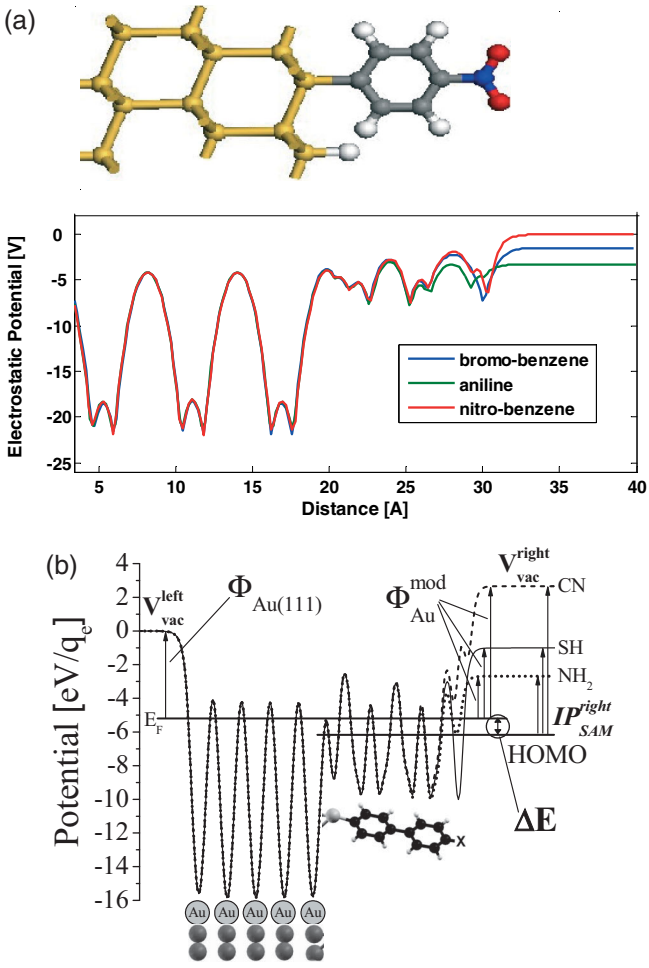

Figure 3. Average electrostatic potential as a function of position inside the structure for a substrate adsorbed with a polar monolayer (at half coverage) with several different polar groups [38,39]. a) Si(111)-adsorbed benzene derivatives, with functional groups of NO_2, Br, and NH_2, adapted from [26]. b) Au(111)-adsorbed 4′-substituted 4-mercaptobiphenyls with functional groups of CN, SH, and NH_2, reproduced from [40], with permission, copyright 2006, American Institute of Physics. Also noted are the Fermi level (E_F) highest occupied molecular orbital (HOMO), and the ionization potential of the modified surface (IP).

the dipole due to the molecule-substrate chemical bond itself has been found, e.g., in the DFT calculations of Rusu and Brocks[43] and Sushko and Shluger.[44] Naturally, this argument can be extended to molecular assemblies possessing several "layers" of polar groups, as has been elaborated by Taylor and Bayes.[45]

It may be prudent at this point to caution against two possible pitfalls in the electrostatic interpretation of DFT calculations. First, if periodic arrays are modeled using a finite cluster, as is often the case in quantum chemistry, then neither Equation 5 nor Equation 9 rigorously holds. Consequently, significant electric fields may be found even when they should be negligible in a continuous layer and the intra-molecular depolarization may not be captured properly due to the absence

of the periodic replicas.[37] The latter observation is consistent with the observation of Cornil et al., who found that a finite cluster should consist of at least tens of molecules for the depolarization to reach its monolayer value.[28] If, instead, periodic boundary conditions are used, this problem obviously does not arise. However, it is important to note that graphical representations of potentials that are laterally averaged over the periodic unit cell, such as those presented in Figure 3, could be misleading. Consider, e.g., the potential given by Equation 9. Because it is, by definition, periodic in x and y, lateral averaging makes all its components except V_{av} (which is the $m = n = 0$ term) vanish at any depth z irrespectively of actual field penetration! In other words, the xy averaged potential outside the dipolar sheet is z-independent. The same is true if the potential of Equation 9 is screened by a uniform dielectric constant throughout the unit cell. The potential changes due to different polar groups, shown in Figure 3, are observed essentially because the dielectric response is not microscopically uniform. Especially for periodic monolayers with low molecular coverage, where significant electric fields can exist deep within the more uniform bulk, lateral averaging can grossly under-represent the extent of field penetration and, similarly, the extent of charge transfer between substrate and molecule.

The preceding arguments highlight intra-monolayer depolarization and a rapid decay of electric fields outside the monolayer as the hallmarks of monolayer electrostatics. Taken together, they allow us to comment on the rationale for and validity of the heuristic Helmholtz equation. This equation relates the potential drop across a polar monolayer, ΔV, to its gas phase dipole, P_0, as:[4,10]

$$\Delta V = 4\pi \frac{NP_0 \cos(\varphi)}{A\varepsilon} \tag{10}$$

where A is the surface area, N is the number of molecules, φ is the molecular tilt angle relative to the surface normal, and ε is an *effective* dielectric constant of the monolayer (not to be confused with the bulk dielectric constant of a molecular solid of the same molecules). Sufficiently far away from the polar monolayer, where all exponential potential terms are negligible, the potential drop across the polar monolayer is given by the difference of V_{av} above and below the monolayer and Equation 8 then yields:

$$\Delta V = \frac{4\pi p_0}{ab(1 + ak/a^3)} \tag{11}$$

If we identify $P_0\cos(\varphi)$, the z-component of the molecular dipole, with the point dipole p_0; A/N, the "footprint" of a single molecule, with the area per point dipole, ab; and ε, the dielectric constant, with the depolarization factor, $1 + ak/a^3$, Equations 10 and 11 become identical. We conclude, then, that the uniform density approximation (namely, the parallel plate capacitor model) works because all potential terms due to non-uniform density components decay exponentially and that the dielectric constant approximation works because it mimics the intra-molecular depolarization. We also note that more elaborate models comprising several capacitors for systems with several dipolar layers and also including image effects have been constructed and applied successfully.[44–48]

Using either Equation 10 or Equation 11, we immediately see how a molecular layer at the surface contributes a potential drop, ΔV, that affects the surface work function and/or electron affinity by $e\Delta V$. Such effects have indeed been observed experimentally for, e.g., Au.[49,50] For semiconductors, a series of studies by Cahen and coworkers,[4,5] showed that the electron affinity of many semiconductors, such as CdTe,[51] CdSe,[52] GaAs,[53] Si,[54] ZnO,[55] and even polycrystalline $CuInSe_2$[50,51] can be changed systematically by adsorbing sets of benzoic and dicarboxylic acid molecules, with varying dipole moments (by changing a given substituent in the molecules) but identical binding to the semiconductor substrates. In these studies, varying the molecular dipoles was achieved mostly by changing the functional group at the top of the monolayer (cf. Fig. 1b). Similar electron affinity modifications were observed for, e.g., TiO_2,[56] In:SnO_2,[57] and SiO_2.[58] Generally, a linear relation exists between changes in the electron affinity and the magnitudes of the gas phase molecular dipoles, as shown in Figure 1b, such that a positive dipole increases the semiconductor electron affinity, whereas the use of a negative molecular dipole decreases it.[59] It should be noted, however, that in many of the above experimental studies, straightforward fitting results in an effective dielectric constant ε that is larger than that expected from molecular depolarization. Possibly, this is because using ε as an empirical fitting parameter allows one to "bury" within it other factors, such as partial coverage, adsorption of foreign molecules (e.g., water), etc.

In a similar vein, Equations 10 and 11 predict that a interfacial dipolar layer can affect the interface dipole and related quantities, such as the Schottky barrier height for metal/semiconductor junctions and the band offset for semiconductor heterojunctions. For example, Campbell et al. have shown that they can control the Schottky barrier between a metal electrode and an organic semiconducting film using self-assembled monolayers.[60] Several studies have shown the ability to control the electrical properties of junctions between metals and inorganic semiconductors by means of adsorbing relatively small organic molecules, such as carboxylic acids on the semiconductor[55,61–63] and cyclic disulfides on the metal side of the interfaces.[64] Examples of junctions that were studied include Au/GaAs (n- and p-type),[61–63] Au/ZnO,[55] Au/Si (with a thin native oxide),[64] and (oxide free) Hg/Si[65] junctions. In most cases, systematic changes in charge transport behavior across the molecularly modified junctions were indeed observed.

Importantly, for monolayers "sandwiched" between a metal and a semiconductor the net interfacial dipole direction can be a strong function of the molecular bond to the substrate and/or the nature and method of deposition of the contact metal.[62] In fact, a comparison of different contacting modes has shown that an intimate contact (i.e., < 1–2 Å proximity) between the molecules' exposed substituents and the (top)

metal contact completely *inverted* the molecular dipole effect on the electrical characteristics of the resulting devices. This behavior was explained by effective dipole inversion due to metal-molecule polarization and partial charge redistribution between metal and molecules[62] (cf. also refs. [66] and [67]). A similar effect, suggesting dipole inversion, was found for Au contacts evaporated indirectly, on a cooled substrate, on a *n*-GaAs substrate bearing a molecular monolayer.[68,69] If Pd was used instead of Au, no such inversion was observed.[68,70] This striking difference was attributed to the difference in growth mechanisms of the Pd and Au films, *viz.*, two dimensional and three dimensional growth, respectively, that leads to differences in the interaction of the metal with the molecules.[69]

Finally, it is well-known that a dipole at a semiconductor-insulator interface of a metal/insulator/semiconductor junction will change the threshold voltage of a field effect transistor based on this structure. This means that this quantity, too, can be controlled by polar organic layers. This has been elegantly demonstrated by Kobayashi et al.,[71] who showed that they could control the surface carrier density in an organic thin film transistor using organosilane self-assembled monolayers sandwiched between the SiO_2 insulator and the active organic film.

3. Electrostatics of Non-ideal Polar Monolayers

Obviously, the perfectly ordered, infinitely periodic molecular monolayer studied in the previous section is an idealization that is rarely encountered in practice. However, as shown above, this does not mean that it cannot capture correctly some of the salient features of realistic monolayers. In this section, we discuss various non-ideal scenarios, with an emphasis on identifying monolayer properties and ensuing device behavior where significant qualitative discrepancies between ideal and real monolayers are expected.

Because organic monolayers often form domains,[72] we start by considering the electrostatics of an ordered array of point dipoles of *finite size*. To understand how the electric field distribution differs from that of an infinite monolayer, we compute the electric field distribution below such an array by numerically superposing the field of each dipole in the array, as given by Equation 1. For simplicity, we again neglect depolarization effects. Note, however, that the depolarization within a finite domain is not uniform because the electric fields at the center and at the edge of the domain are not the same, as elaborated below. This can make a quantitative difference, but can be neglected to first order for a discussion of qualitative features.[73]

Several different views of an instructive example – rectangular finite domains of various sizes, each consisting of the same dipoles as studied in Figure 2 – are given in Figure 4.

The electric field distributions due to finite dipolar domains with dimensions of 60×60 Å^2, 120×120 Å^2, and 240×240 Å^2 are given in Figure 4a and b, respectively, for planes lying 10 Å and 100 Å below the dipolar layer. At 10 Å below the dipolar layer, there is a pronounced edge effect, similar to that of a classical plate capacitor: The field is stronger at the edge and is by-and-large independent of the domain size. The field decays towards the center of the domain. At the center, the electric field value is smaller the larger the domain is. At 100 Å below the dipolar layer, a different picture emerges: the field is more uniform, it increases with increasing domain size, and it shows larger values below the center than below the edges. More insight into these profound differences can be gained from inspecting Figure 4c, which shows the distribution of the magnitude of the total electric field at the domain center and the (center of the) domain edge for three different finite dipolar domains, with lateral dimensions of 84×84 Å^2, 900×900 Å^2, and 9000×9000 Å^2. At one extreme, close to the dipolar layer the electric field at the domain center (solid line) does not differ appreciably from the exponentially decaying field of an infinite dipolar layer (dotted line). This is because in this "near field" regime, the termination of the domain is "too far" to have an appreciable effect. Naturally, the larger the domain is the larger the extent of the "near field" regime is (one can say that for an infinite layer, the electric field is always at the "near field" regime). At the other extreme, at large distances the electric field at the center of the domain attains a "far field" asymptotic behavior (dashed lines), where the field scales as $1/r^3$ and the domain can essentially be thought of as a single dipole at the origin, whose magnitude is the simple sum of all the individual dipoles. Naturally, the larger the domain is, the further away the onset of the "far field" regime appears.

As expected, Figure 4c reveals a large intermediate range where neither limit applies. On the one hand, the cancellation of the contributions of different dipoles, which is at the heart of the exponential decay for an infinite monolayer, is far from complete. On the other hand, the variation in distances to individual dipoles is too large to view them as one large, "merged" point dipole. The figure also reveals that the electric field at the center of the domain is nearly constant – and not necessarily negligible – over most of the intermediate range. Because the cross-over from the intermediate to the "far field" regime takes place when the solid angle at which the domain is viewed is at some critical angle, the "far field" limit for any domain, with a length D on each side, is attained at a height (z) with a fixed z/D ratio. At that point, the magnitude of the electric field is of the order of p/z^3, where p, the overall dipole, scales as $\sim D^2$. Thus, at the cross-over point and throughout the "nearly constant" regime, the electric field scales as $1/D$. In other words, the "plateau" in Figure 4c is inversely proportional to the domain size.

Importantly, the electric field at the edge of the domain (dash-dotted lines in Fig. 4c) is significantly larger than the field at the center upon departure from the "near field" regime. It decreases approximately as $\sim 1/r$, eventually becoming smaller than the field at the center before they both merge at the "far field" limit. However, the direction of the electric field at the center and at the edge is not the same. Figure 4d

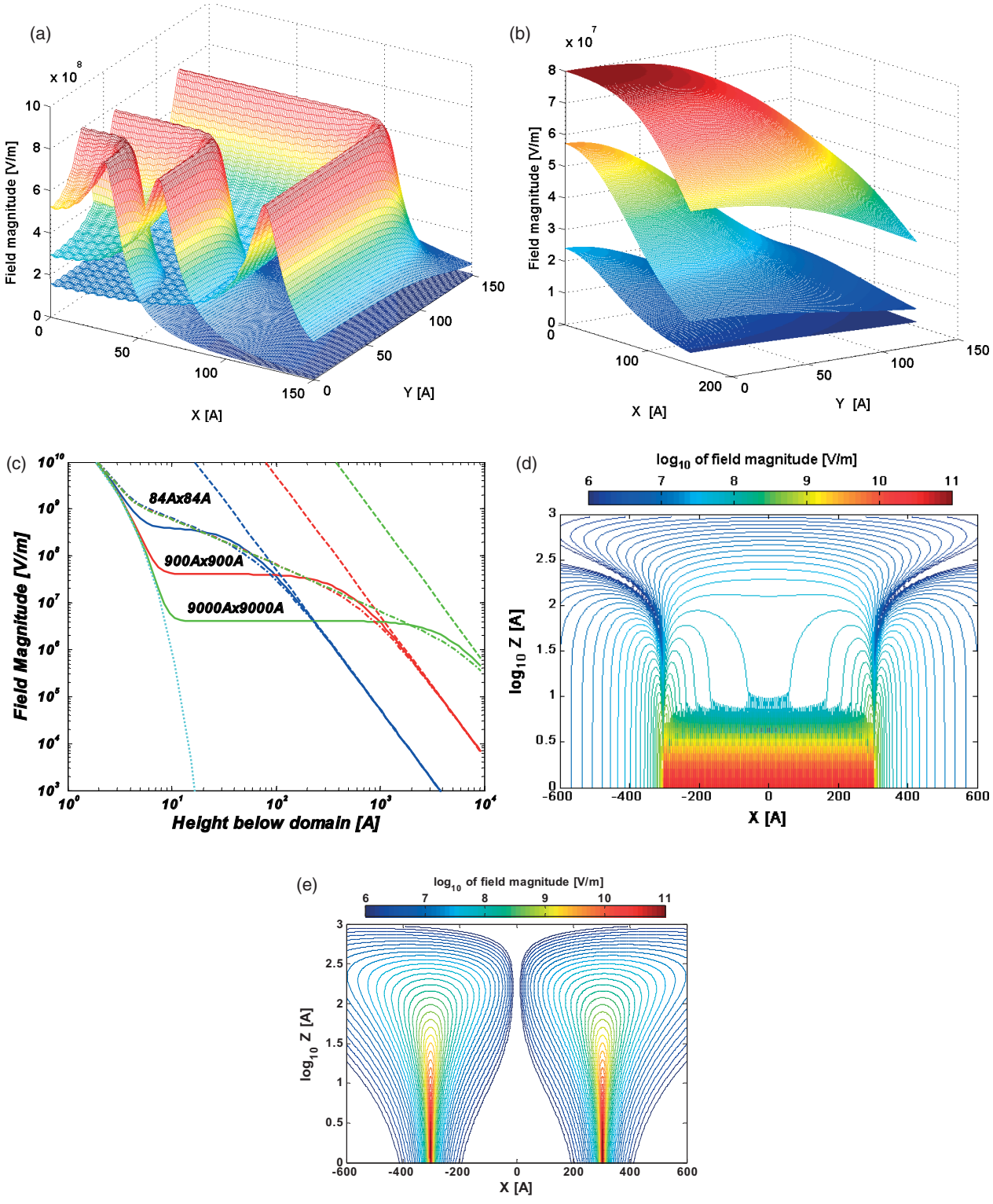

Figure 4. Several different perspectives on the electric field distribution due to a finite square arrays of $p = 4$ Debye, $d = 2$ Å dipoles with inter-dipole separation of $a = b = 6$ Å**. a)** Distribution of the magnitude of the total electric field in the *xy* plane (with the domain center at $x = y = 0$), at a distance of 10 Å ("near field") below dipolar arrays with overall lateral dimensions of 60 × 60 Å^2, 120 × 120 Å^2, and 240 × 240 Å^2. b) same as (a), but at a distance of 100 Å below the layer ("far field"). c) Magnitude of the total electric field as a function of distance below the domain, *z*, for dipolar arrays with overall lateral dimensions of 84 × 84 Å^2, 900 × 900 Å^2, and 9000 × 9000 Å^2, at the domain center (solid lines) and below the center of its edge (dash-dotted lines). Note that all dash-dotted lines converge for small enough *z* values. Also shown are the "near field" (dotted line) and "far field" (dashed lines) asymptotic curves. d) Contour plot of the distribution of the *z*-component of the electric field at the *xz* plane, for a 600 × 600 Å^2 finite array. e) Same as (d), for the *x*-component of the electric field.

ADVANCED MATERIALS

and e provide contour plots for the z-component and the x-component, respectively, for a 600 × 600 Å^2 domain. From symmetry argument, at the center of the domain the field must be in the z direction. But as one moves towards the edge, the x-component of the electric field becomes larger and eventually dominates. Near the edge of the domain, then, the absence of "left-right" cancellation of dipoles is more pronounced than the absence of "near-far" cancellation. This is reasonable, because at the edge all dipoles are either "left" or "right", but some are still "near" and some "far".

The above-elaborated behavior of the rectangular domain is qualitatively typical to domains whose extent in both lateral directions is similar. Consider, however, a rectangular domain of lateral dimensions $a \times b$, such that $a >> b$, the most extreme case of which is a one-dimensional finite dipolar line. From Gauss' law, the electric field outside a charged *wire* (as opposed to plate) with a uniform one-dimensional charge density, λ, is $E_r = \lambda/2\pi r$. Taking two such wires, separated by a distance d, we obtain, for $d \to 0$, that E_z straight above the two wires is given by $p/2\pi r^2$, where p is the one-dimensional dipole density. This is fundamentally different than the previous case (but note that numerical calculations show that edge behavior is similar in the two systems).

It is also very important to consider a different kind of domains, where molecules are *absent* from a region of adsorption sites, a process which often occurs naturally in monolayers.[72] From an electrostatic perspective, the superposition principle tells us that electric field due to an otherwise ideal dipolar monolayer with a "pinhole" is simply the difference between the electric field of the perfect monolayer and the electric field of the "missing domain". This is illustrated in Figure 5 for the simplest "missing domain" possible – a single missing dipole. Because the field of the perfect monolayer decays rapidly, at vertical distances of the order of the lateral distance between dipoles the electric field is very similar to that of a single dipole in the *opposite* direction. This is straightforward from the electrostatics point of view, but has interesting chemical consequences: Assuming a fixed binding group, the electric field "felt" by the substrate due to a finite-domain of molecules with a strongly electron-donating group and that due to a hole-possessing monolayer with a strongly electron-withdrawing group, are essentially the same if the "hole" and the domain are of the same dimensions. This is so even though the modification of the work function are of opposite sign in the two cases.

Interestingly, finite-domain electrostatic effects of the type shown in Figures 4 or 5 will not be captured by DFT calculations of either a single (or a few) molecules on a cluster or of an ideal periodic monolayer. If we wish to include such effects within a DFT calculation without explicitly computing the electronic structure of at least hundreds or possibly thousands of molecules, the proper electrostatic regime will have to be enforced by adding additional terms to the Hamiltonian. To the best of our knowledge, this has not been done.

Turning our attention to experiment, one striking example where the experimentally observed behavior of an electronic

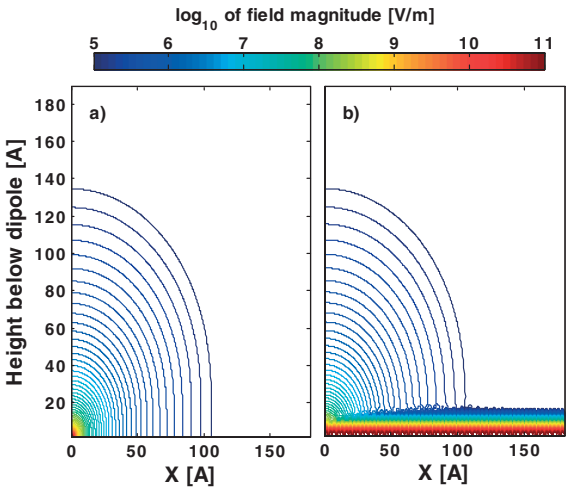

Figure 5. Distribution of the electric field magnitude, on a logarithmic scale, in the xz plane due to: a) A single dipole with p = 4 Debye and d = 2 Å; and b) A square array of such dipoles with inter-dipole separation of $a = b$ = 6 Å, with the dipole at $x = y = 0$ missing.

device cannot be reconciled even qualitatively with the properties of *ideal* monolayers, but are well explained by considering *non-ideal* monolayers, is found in the study of metal-semiconductor junctions possessing a molecularly-modified interface.[19,63,74,75] Here, we examine the Au/(CH_3-terminated dicarboxylic acid)/n-GaAs junction, where Au is gently evaporated on the n-GaAs substrate bearing molecular monolayer, as a prototypical case.[76] For this system various measurements, e.g., quantitative x-ray photoelectron spectroscopy (XPS) and Fourier transform infrared spectroscopy (FTIR) confirmed that the (top) contact-free molecular monolayer is *discontinuous*. That this is also the case also with an applied top contact was confirmed by ballistic electron emission microscopy (BEEM) as shown in Figure 6.[75]

A comparison of conventional STM topography of the Au/*n*-GaAs junction, with or without the interfacial molecular monolayer (Fig. 6a and c) reveals a similar Au grain structure. The simultaneously-measured BEEM current map, however, reveals relatively small (mostly < 3 pA) spatial variations in the current amplitude that are strongly correlated with the polycrystalline grain structure of the Au film of the bare Au/n-GaAs sample (Fig. 6b), but not with that of the molecularly modified one (Fig. 6d). In the latter case, the BEEM current is extremely small over most of the image area, except at isolated bright patches that are ~ 20 nm across in size. Schottky Barrier heights (SBH), extracted at various lateral positions in both samples, are consistent with these current-map-based observations. Analysis of BEEM current-voltage curves at various lateral locations shows that for the bare Au/n-GaAs sample the SBH is quite uniform, with a mean of ~ 0.92 eV and a standard deviation of ~0.02 eV. For the monolayer-inserted Au/n-GaAs sample, the local SBHs measured at 10 different pinholes were found to have a mean value of ~ 0.95 eV with a standard deviation of ~ 0.03 eV. These values were

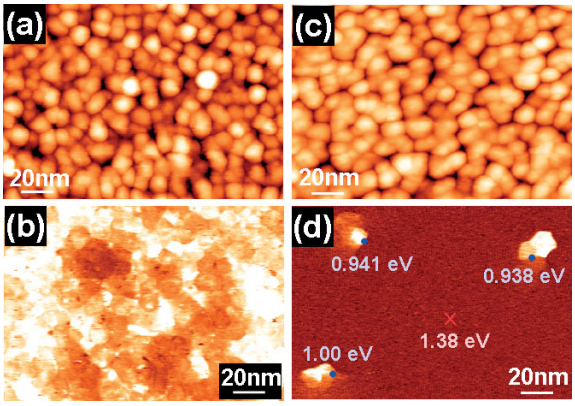

Figure 6. a) STM and b) simultaneous BEEM image (measured at an STM tip bias of 1.2 V) of a "bare" Au/*n*-GaAs sample, i.e., without a molecular monolayer. Color scales are 3.4 nm and 3 pA, respectively. c) STM and d) simultaneous BEEM image (measured at an STM tip bias of 1.38 V) of a Au/(CH_3-terminated dicarboxylic acid)/n-GaAs sample. Color scales are 3.6 nm and 1 pA, respectively. Numbers in Gray are local Schottky barrier heights and the number in red is the applied bias. Reproduced from [75], with permission).

largely in agreement with those previously estimated for similar samples using macroscopic temperature-resolved current-voltage, capacitance-voltage, and internal photoemission spectroscopy measurements.[19] Because the molecule studied is expected to increase the Schottky barrier height (SBH), as well as to pose an additional tunneling barrier to current, the BEEM results strongly suggest that (at least for the tip bias used) the current flowing directly through the molecular monolayer is negligible. Instead, significant current flows only through ~ 20 nm size pinholes in the monolayer, where a direct Au/n-GaAs contact is established.

The main reason for the drastic reduction in junction current over the interface areas with the molecular layer present is likely the low transmission coefficient of carriers across molecules.[77] Because most current across the Au/(dicarboxylic acid)/n-GaAs interface has passed through small areas devoid of molecules, it may seem that the dipole moment of the molecular layer is irrelevant for current transport. However, the experimental data show that the effective SBH for pinhole conduction has been influenced by the dipole of the molecular layer, possibly due to the edge effects elaborated in Figure 4. Effectively, the conduction path through the (semiconductor below the) pinhole is "gated" by fringing electric field from the surrounding molecular layer.[78,79] If the polarity of the molecular dipole is such that it increases the SBH, as in Figure 6, the effect of the molecular layer is equivalent to a "reverse gate bias" applied to the pinhole conduction path. This makes the *effective* SBH for the pinhole larger, in agreement with experiment. Clearly, the effect can become negligible for sufficiently large pinholes. Conversely, for small enough pinholes dipoles of the molecular layer can effectively "pinch-off"[80] the current through the pinhole.[81]

We point out that the pinch-off of current through low-resistance patches of a metal-semiconductor junction is not limited to those with partial molecular dipole layers inserted at the interface. It is known that the current transport across bare Schottky barriers, which are fabricated (intentionally or unintentionally) with spatially inhomogeneous barrier height, can also be significantly influenced by the potential "pinch-off" effect.[78] The conduction paths in front of low-barrier-height patches can exhibit band-bending due to the presence of high-barrier-height region in close proximity. This electrostatic phenomenon, which is of the same nature as that presently discussed for molecular dipole layers, is well understood experimentally and theoretically for inhomogeneous Schottky barriers, and has been discussed in ref. [78]. Interestingly, the modeling of the band-bending at inhomogeneous, but bare, Schottky barriers was most conveniently carried out by assuming the presence of an inhomogeneous dipole layer at the interface, reminiscent of the morphology of partial molecular dipole layer in our discussion. That simple model then led to analytic expressions for the inhomogeneous Schottky barriers which were found to be in agreement with experimental data and computer simulation results.

A different type of electronic device that is dominated by electrostatic effects in dipolar layers is the FET-like structures that are used for sensing chemical processes. Such devices are generally known as CHEMFETs. There are many different varieties of CHEMFETS (see, e.g., refs. [82–84] for overviews), most of which, however, are loosely based on the same principle: The presence of molecules or ions influences the potential of the conducting FET channel either by directly influencing the gate potential (e.g., for a catalytically active metal gate) or by changing the potential distribution between a "reference electrode gate" and the semiconductor. As is often the case in electronic devices (e.g., with the concept of doping), extremely small chemical perturbations can have large electrical consequences. This means that properly designed CHEMFETs are sensitive to, and can be used to detect, minute concentrations of chemicals. In CHEMFETs with a reference gate, even an ideal polar layer can induce a significant field in the channel.[85,86] This field ensues because the overall potential difference between the ground and the reference electrode must remain the same with or without the polar layer, i.e., fields external to the dipole layer must be induced so as compensate for the potential drop on it[10] (the same reasoning applies to the results of Kobayashi et al.,[71] discussed at the end of the previous section).

Chemical sensing with FETs *having no reference electrode*, shown schematically in Figure 7, relies on a somewhat different mechanism. Such devices have generally been referred to as molecularly controlled semiconductor resistors (MOCSERs).[17] In MOCSERs, the traditional gating electrode is either present at the back, with a molecular layer adsorbed directly on the semiconductor (Fig. 7a),[18] or is replaced altogether by a molecular layer adsorbed on a (typically ultrathin) dielectric (Fig. 7b).[16] In either configuration, binding molecules from the gas or liquid phase to the "chemical sensing molecules" changes the potential in the conducting channel. Consequently, the current between source and drain is

ADVANCED MATERIALS

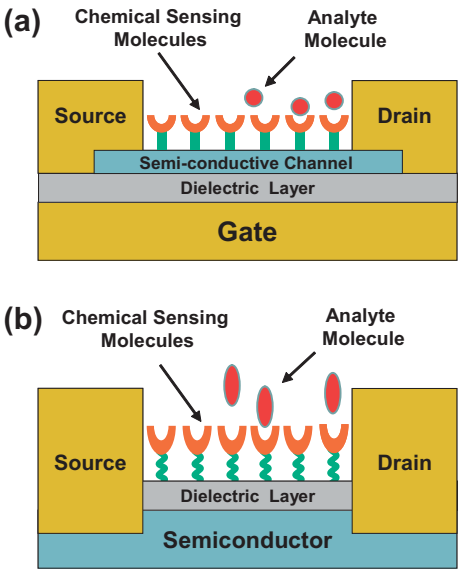

Figure 7. Schematic representation of MOCSER structures used for chemical sensing without a reference electrode: a) the molecular layer is adsorbed directly on the semiconductor and the gating is done from the back. b) the FET gate is replaced by a molecular layer adsorbed on the (thin) dielectric.

modified and the device serves as a sensor. Such devices can have high chemical sensitivity. For example, a GaAs-based MOCSER with a monolayer of suitable porphyrins was used successfully to detect ~ppb concentrations of NO in both physiological solution[16,86] and in air.[87] A high-sensitivity MOCSER based on GaN/AlGaN has been similarly used for polar liquid sensing.[88]

The pertinent question for our discussion is the mechanism through which the potential in the conductive channel is modified by adsorption of a polar layer on a MOCSER. In either a CHEMFET or a MOCSER (i.e., with or without a reference electrode, respectively), if charged species are adsorbed, or if the surface is effectively charged upon adsorption, then potential modifications at the channel necessarily take place, from an electrostatic point of view. However, the homogeneous adsorption of a layer of polar yet neutral molecules on the device structures of Figure 7 has no first order effect on the electrostatics of the conduction channels, based on the arguments of Section 2. Therefore, one would not expect the adsorption of an ideal polar monolayer to be detectable in structures without reference gates. Nevertheless, the detection of the changes in the dipole moment of a functional group by MOCSERs has been observed experimentally. Clear-cut evidence for this was recently provided by He et al.[18] Using a device structure as in Figure 7a, they showed a distinct correlation between the threshold voltage of the FET and the polarity of the functional group for molecules of the type shown in Figure 3a. For device structures as shown in Figure 7b, Rudich et al.[89] found that adsorption of a small fraction (~ 10 %) of either H_2O or O_2 on a MOCSER, with a channel covered by a monolayer of alkyl chains, yielded very large signals, but in opposite directions. This has also been interpreted in terms of opposite directions of the dipole moment induced in the monolayer upon adsorption of the detected species.[17] Likewise, the above-mentioned work on NO detection[16,86] has been discussed in terms of induced dipoles, rather than adsorption of charged species.

One plausible explanation of the observed results seems to be that the residual fields outside the (uniform) dipole layer are still sufficient to induce a very small degree of charge transfer between substrate and organic layer. The net charge due to this transfer could then modulate the field in the channel.[17] He et al. estimated the changes in charge transfer between different benzene derivatives to be of the order of ~ 10^{-3} e.[18] Similar numbers were indeed found in the DFT calculations of Natan et al.[27] Although this is a minute charge from a chemical point of view, it is large in electrical terms and would seem to be amenable to detection. However, the fields associated with such charge transfer are still those of a *dipole* rather than of a *monopole*. Thus, the observed current modulation in conduction channels whose depth below the surface is large compared to the inter-molecular spacing is still left unaccounted for.

It seems that in these devices issues of practical, non-ideal monolayers have to be considered. One such issue that we have not considered so far is that of surface states, which naturally arise at any surface which is not perfectly passivated (see, e.g., ref. [10] for a detailed discussion). Such states provide a *monopolar* surface charge density. Cohen et al. have shown experimentally that, for a variety of semiconductors, adsorption of molecules possessing the same binding group but different polar groups may significantly change the surface band bending by modifying the surface state distribution.[14] This was interpreted in terms of frontier orbital interaction[90] between the surface states of the substrate and the lowest unoccupied molecular orbital of the molecule. Such modification of surface states could well cause the above-mentioned relatively minute change in monopolar charge required to drive the MOCSER. Even if surface states are not an issue, one should recall that the entire MOCSER device has a finite lateral extent and is therefore a finite domain in the sense discussed above. Furthermore, even if the "chemical sensing monolayer" is ideal, the picture of an ideal layer of analyte molecules adsorbing on the surface like a spread-out blanket descending on a mattress is clearly unrealistic. Thus, in addition to the inherent non-ideality of the chemical sensing monolayer, there will be additional non-ideality induced by partial adsorption, generating smaller polar domains inside the active area of the device. In either case, Figure 4 then immediately leads to non-negligible fields that can appear at appreciable depths inside the MOCSER structures and ergo generate meaningful signals.

To the best of our knowledge, this reasoning has not been explored quantitatively yet and we are not aware of experiments where the MOCSER signal was studied as a function of a well-controlled device size, degree and pattern of surface coverage, and channel depth for a well-passivated surface. In-

terestingly, Wu et al.[86] found that the MOCSER signal with a mixed hemin/benzoic acid layer gave a much stronger response signal to NO than a device with a pure hemin monolayer, even though NO is only adsorbed on the hemin molecules. Possibly, this is simply because adding the carboxylate spacer enhances the NO binding rate to the hemin (a fact also evident from the shorter time constant found with the spacer). However, atomic force microscopy (AFM) images on mica revealed a clear domain pattern of adsorption with the carboxylate spacer and this may also serve to explain the enhanced signal.

In the context of both the molecularly modified Schottky-diodes and the MOCSER devices, another possible degree of freedom in device design is that of deliberate patterning, namely the engineering of domains possessing polar molecules and domains devoid of them, e.g., by modern lithography techniques. The Fourier spectrum of the charge distribution of such a pattern would be a convolution between the Fourier spectrum of the pattern function and the Fourier spectrum of the ideal monolayer.[91] This will necessarily lead to long-range lateral Fourier components that, in analogy to Equation 9, would lead to large vertical decay lengths. Naturally, for MOCSER applications one would need to explore the effect of significant lateral variations in channel potential on the device performance.[78,79]

Before concluding this section, we note that recently there has been much experimental interest in molecular sensors based on molecule adsorption on nano-wires (e.g., refs. [92–95]) or (semiconducting) nano-tubes (e.g., refs. [96–98]). In 1d systems, as in the 2d systems studied above, the behavior of an ideal molecular layer can be approximated to zero order by a capacitor, except that here it is a parallel cylinder rather than a parallel plate capacitor. Still, there would be no electric field outside the "capacitor", i.e., inside the nano-wire. Arrangements of point dipoles with cylindrical symmetry can be treated, similar to procedures given in Equations 7–9, in cylindrical coordinates. This leads to a Fourier–Bessel expansion for the potential.[21] The sum of decaying exponentials is replaced by a sum of decaying modified Bessel functions, where again the decay is of the order of the inter-molecular distance. The less dense coverage along the cylinder diameter is, the larger the decay length of the electric field into the nano-wire is. The crucial difference from the 2d cases we analyzed so far, however, is that the active cross-section of the device is inherently smaller. This is obviously true for a nano-tube, where only one, or a few, substrate "monolayers" exist. But even in a nano-wire, the portion of the "substrate" influenced by the electric fields can be much greater than in a 2d device.[99]

4. Concluding Remarks

In this article, we have analyzed the effect of both ideal and non-ideal polar monolayers on electronic devices entirely in terms of classical electrostatics. We have shown that very simple considerations can in fact be highly predictive for a wide range of seemingly different phenomena. Most importantly, we have shown that the analysis of infinitely periodic polar monolayers explains modifications of surface and interface potentials, whereas the analysis of finite-domain monolayers readily explains experimentally observed field effects, unexpected from ideal monolayers. Note, however, that we made no attempt to incorporate either thermodynamic or kinetic considerations that would, predict, e.g., driving forces for domain formation. Instead, we focused on the electric consequences of an already-formed ideal or non-ideal monolayer.

It may appear surprising that classical theory is sufficient to describe the dominant phenomena in what is obviously a complicated quantum system. This is rationalized by invoking Kohn's "near-sightedness principle" of quantum mechanics.[100] According to this principle, perturbation of the external potential at a distant region from a given location generally has a small effect on any static property of a many-particle system at that location. This means that outside the immediate vicinity of the dipole, "near-sightedness" prevails and detailed quantum mechanical considerations are no longer necessary.

Specifically, *long-range electric fields are an exception to the "near-sightedness principle"*.[100] This fact is cardinal to the analysis performed in this paper. First, it is the fundamental reason why away from the monolayer it is sufficient to consider electric fields, the treatment of which is handled very well by classical theory. Second, it is responsible for the breakdown of the assumption tacitly made in many chemical analyses, i.e., that all system properties are controlled by the local chemical environment. This is precisely why we witness such strong "cooperative field effects",[17] i.e., field effects that are determined by the entire *ensemble* of polar molecules, rather than solely by the properties of the individual molecules.

Quantum mechanics is, however, crucial for understanding properties determined by local interactions, i.e., the gas phase dipole of the polar molecule and its possible modification upon bonding to a substrate and/or an overlayer. For example, the dipole inversion upon deposition of a top metal contact,[62] discussed in Section 2, is certainly outside the scope of classical electrostatics. Moreover, sufficiently strong "cooperative field effects" can, in turn, affect local properties to the extent that quantum mechanics is needed again. For example, for highly polar molecules, it is in fact not at all obvious that a molecular monolayer would form, because of the energy penalty associated with packing a polar monolayer due to the repulsive dipole-dipole interactions.[24] And even if such a layer does form, the strong electric fields within it may cause a complete rearrangement of the molecular electronic structure by changing the energy landscape to the extent that the gas phase energy minimum is no longer relevant.[101] In such cases, a detailed treatment of all energy components, including all molecule-substrate and molecule-molecule interactions, *in the new ground-state*, is necessary before application of the electrostatic theory presented in this theory is meaningful.

In conclusion, we hope to have elucidated the interplay between local chemical structure and global geometric consid-

ADVANCED MATERIALS

erations, as mediated by long-range electric fields. We also hope to have explained how this interplay manifests itself in practical electronic devices and to have provided tools for the analysis and considerations for the design of molecular monolayers for controlling such devices.

Received: July 11, 2007
Revised: August 29, 2007

[1] *Molecular Electronics: Science and Technology* (Eds: A. Aviram, M. Ratner), New York Academy of Sciences, New York **1999**.
[2] J. R. Heath, M. A. Ratner, *Physics Today* **2003**, *56*, 43.
[3] *Introducing Molecular Electronics* (Eds: G. Cuniberti, G. Fagas, K. Richter), *Springer, Berlin* **2005**.
[4] G. Ashkenasy, D. Cahen, R. Cohen, A. Shanzer, A. Vilan, *Acc. Chem. Res.* **2002**, *35*, 121.
[5] A. Vilan, D. Cahen, *Trends Biotechnol.* **2002**, *20*, 22.
[6] B. O'Reagan, M. Grätzel, *Nature* **1991**, *353*, 737.
[7] J. J. Wei, C. Schafmeister, G. Bird, A. Paul, R. Naaman, D. H. Waldeck, *J. Phys. Chem. B* **2006**, *110*, 1301.
[8] a) Z. Vager, R. Naaman, *Chem. Phys.* **2002**, *281*, 305. b) I. Carmeli, V. Skakalova, R. Naaman, Z. Vager, *Angew. Chem. Int. Ed.* **2002**, *41*, 761.
[9] P. Crespo, R. Litrán, T. C. Rojas, M. Multigner, J. M. de la Fuente, J. C. Sánchez-López, M. A. García, A. Hernando, S. Penadés, A. Fernández, *Phys. Rev. Lett.* **2004**, *93*, 087204.
[10] L. Kronik, Y. Shapira, *Surf. Sci. Rep.* **1999**, *37*, 1, Sections 2.1.4, 2.1.5, and 5.2.
[11] B. D. Campbell, H. E. Farnsworth, *Surf. Sci.* **1968**, *10*, 197.
[12] A. Franciosi, C. G. Van de Walle, *Surf. Sci. Rep.* **1996**, *25*, 1.
[13] a) T. dell'Orto, J. Almeida, C. Coluzza, A. Baldereschi, G. Margaritondo, M. Cantile, S. Yildirim, L. Sorba, A. Franciosi, *Appl. Phys. Lett.* **1994**, *64*, 2111. b) M. Marsi, R. Houdre, A. Rudra, M. Ilegems, F. Gozzo, C. Coluzza, G. Margaritondo, *Phys. Rev. B* **1993**, *47*, 6455.
[14] a) R. Cohen, L. Kronik, A. Shanzer, D. Cahen, A. Liu, Y. Rosenwaks, J. K. Lorenz, A. B. Ellis, *J. Am. Chem. Soc.* **1999**, *121*, 10545. b) R. Cohen, L. Kronik, A. Vilan, A. Shanzer, Y. Rosenwaks, D. Cahen, *Adv. Mater.* **2000**, *12*, 33.
[15] I. Higuchi, T. Ree, H. Eyring, *J. Am. Chem. Soc.* **1955**, *77*, 4969.
[16] D. G. Wu, G. Ashkenasy, D. Shvarts, R. V. Ussyshkin, R. Naaman, A. Shanzer, D. Cahen, *Angew. Chem. Int. Ed.* **2000**, *39*, 4496.
[17] D. Cahen, R. Naaman, Z. Vager, *Adv. Funct. Mater.* **2005**, *15*, 1571.
[18] T. He, J. He, M. Lu, B. Chen, H. Pang, W. F. Reus, W. M. Nolte, D. P. Nackashi, P. D. Franzon, J. M. Tour, *J. Am. Chem. Soc.* **2006**, *128*, 14537.
[19] H. Haick, M. Ambrico, T. Ligonzo, R. T. Tung, D. Cahen, *J. Am. Chem. Soc.* **2006**, *128*, 6854.
[20] See, e.g., a) G. P. Srivastava, *Theoretical Modeling of Semiconductor Surfaces: Microscopic Studies of Electrons and Phonons*, World Scientific, Singapore **1999**. b) G. P. Srivastava, *Rep. Prog. Phys.* **1997**, *60*, 561.
[21] See, e.g., J. D. Jackson, *Classical Electrodynamics*, 2nd ed., Wiley, New York **1975**.
[22] J. R. MacDonald, C. A. Barlow, Jr., *J. Chem. Phys.* **1963**, *39*, 412.
[23] J. Topping, *Proc. R. Soc. London Ser. A* **1927**, *114*, 67.
[24] a) O. Gershevitz, C. N. Sukenik, J. Ghabboun, D. Cahen, *J. Am. Chem. Soc.* **2003**, *125*, 4730. b) O. Gershewitz, M. Grinstein, C. N. Sukenik, K. Regev, J. Ghabboun, D. Cahen, *J. Phys. Chem. B* **2004**, *108*, 664.
[25] H. Fukagawa, H. Yamane, S. Kera, K. K. Okudaira, N. Ueno, *Phys. Rev. B* **2006**, *73*, 041302.
[26] A. Natan, Y. Zidon, Y. Shapira, L. Kronik, *Phys. Rev. B* **2006**, *73*, 193310.
[27] V. De Renzi, R. Rousseau, D. Marchetto, R. Biagi, S. Scandolo, U. del Pennino, *Phys. Rev. Lett.* **2005**, *95*, 046804.
[28] D. Cornil, Y. Olivier, V. Geskin, J. Cornil, *Adv. Funct. Mater.* **2007**, *17*, **1143.**
[29] G. Heimel, L. Romaner, E. Zojer, J.-L. Brédas, *Nano Lett.* **2007**, *7*, 932.
[30] V. Perebeinos, M. Newton, *Chem. Phys.* **2005**, *319*, 159.
[31] L. Segev, A. Salomon, A. Natan, D. Cahen, L. Kronik, F. Amy, C. K. Chan, A. Kahn, *Phys. Rev. B* **2006**, *74*, 165323.
[32] M. L. Sushko, A. L. Shluger, *J. Phys. Chem. B* **2007**, *111*, 4019.
[33] J. E. Lennard-Jones, M. Dent, *Trans. Faraday Soc.* **1928**, *24*, 92.
[34] In Equations 7 and 9 the potential is expressed using complex notation for convenience. However, the result is necessarily real because the contributions from the m,n and $-m,-n$ terms in the summation are so that the imaginary part is zero.
[35] Obtaining the limit involves a step where the term $\sqrt{(m/a)^2+(n/b)^2}d$ is taken to zero when d tends to zero. This is *not* a valid limit for an arbitrary m,n pair as these Fourier indices can be arbitrarily large. However, because of the exponential decay in z, one can always find an m,n pair of values such that all potential terms above it are arbitrarily small. Therefore, the limit needs to be taken in practice only for finite values of m,n and is therefore correct.
[36] See, e.g., F. J. Zucker, Robert E. Collin, *Antenna Theory*, McGraw-Hill, New York **1969**.
[37] D. Deutsch, A. Natan, Y. Shapira, L. Kronik, *J. Am. Chem. Soc.* **2007**, *129*, 2989.
[38] Note that details of the electrostatic potential near the nuclei differ in parts (a) and (b) of Figure 3. This is merely a consequence of whether the electrostatic potential is computed directly (as in b) or derived from the computed dipole (as in a). This difference is a technical consequence of the use of pseudopotentials and bears no physical significance for the present discussion. For elaboration, see Section 4 of ref. [39].
[39] A. Natan, L. Kronik, Y. Shapira, *Appl. Surf. Sci.* **2006**, *252*, 7608.
[40] G. Heimel, L. Romaner, J.-L. Brédas, E. Zojer, *Phys. Rev. Lett.* **2006**, *96*, 196806.
[41] G. Heimel, L. Romaner, J.-L. Brédas, E. Zojer, *Surf. Sci.* **2006**, *600*, 4548.
[42] N. K. Adam, J. F. Danielli, J. B. Harding, *Proc. R. Soc. London Ser. A* **1934**, *147*, 491.
[43] a) P. C. Rusu, G. Brocks, *J. Phys. Chem. B* **2006**, *110*, 22628. b) P. C. Rusu, G. Brocks, *Phys. Rev. B* **2006**, *74*, 073414.
[44] M. L. Sushko, A. L. Shluger, unpublished.
[45] D. M. Taylor, G. F. Bayes, *Phys. Rev. E* **1994**, *49*, 1439.
[46] J. Demchak, T. Fort, Jr., *J. Colloid Interface Sci.* **1974**, *46*, 191.
[47] P. Dynarowicz-Latka, A. Cavalli, D. A. S. Filho, P. Milart, M. C. dos Santos, O. N. Oliveira, *Chem. Phys. Lett.* **2001**, *337*, 11.
[48] M. Iwamoto, Y. Mizutani, A. Sugimura, *Phys. Rev B* **1996**, *54*, 8186.
[49] a) S. D. Evans, A. Ulman, *Chem. Phys. Lett.* **1990**, *170*, 462. b) S. D. Evans, E. Urankar, A. Ulman, N. Ferris, *J. Am. Chem. Soc.* **1991**, *113*, 4121.
[50] M. Bruening, R. Cohen, J.-F. Guillemoles, T. Moav, J. Libman, A. Shanzer, D. Cahen, *J. Am. Chem. Soc.* **1997**, *119*, 5720.
[51] M. Bruening, E. Moons, D. Yaron-Marcovich, D. Cahen, J. Libman, A. Shanzer, *J. Am. Chem. Soc.* **1994**, *116*, 2972.
[52] M. Bruening, E. Moons, D. Cahen, A. Shanzer, *J. Phys. Chem.* **1995**, *99*, 8368.
[53] S. Bastide, R. Butruille, D. Cahen, A. Dutta, J. Libman, A. Shanzer, L. Sun, A. Vilan, *J. Phys. Chem.* **1997**, *101*, 2678.
[54] R. Cohen, N. Zenou, D. Cahen, S. Yitzchaik, *Chem. Phys. Lett.* **1997**, *279*, 270.
[55] A. Salomon, D. Berkovich, D. Cahen, *Appl. Phys. Lett.* **2003**, *82*, 1051.
[56] J. Kruger, U. Bach, M. Grätzel, *Adv. Mater.* **2000**, *12*, 447.
[57] a) L. Zuppiroli, L. Si-Ahmed, K. Kamaras, F. Nüsch, M. N. Bussac, D. Ades, A. Siove, E. Moons, M. Grätzel, *Europhys. J. B* **1999**, *11*, 505. b) F. Nüsch, F. Rotzinger, L. Si-Ahmed, L. Zuppiroli, *Chem.*

Phys. Lett. **1998**, *288*, 861. c) C. Ganzorig, K.-J. Kwak, K. Yagi, M. Fujihira, *Appl. Phys. Lett.* **2001**, *79*, 272
[58] a) Y. Ofir, N. Zenou, I. Goykhman, S. Yitzchaik, *J. Phys. Chem. B* **2006,** *110,* 8002. b) R. Sfez, N. Peor, S. R. Cohen, H. Cohen, S. Yitzchaik, *J. Mater. Chem.* **2006**, 16, 4044.
[59] By definition, the dipole moment is a vector oriented from the negative to the positive pole. Here, we define a dipole as negative if its negative pole is closer to the semiconductor surface and positive if the negative pole. Note that sometimes the opposite definition is adopted.
[60] a) I. H. Campbell, J. D. Kress, R. L. Martin, D. L. Smith, *Appl. Phys. Lett.* **1997**, *71*, 3528. b) I. H. Campbell, S. Rubin, T. A. Zawodzinski, J. D. Kress, R. L. Martin, D. L. Smith, N. N. Barashkov, J. P. Ferraris, *Phys. Rev. B* **1996**, *54*, R14321.
[61] A. Vilan, A. Shanzer, D. Cahen, *Nature* **2000**, *404*, 166.
[62] A. Vilan, J. Ghabboun, D. Cahen, *J. Phys. Chem. B* **2003**, *107*, 6360.
[63] H. Haick, M. Ambrico, T. Ligonzo, D. Cahen, *Adv. Mater.* **2004**, *16*, 2145.
[64] Y. Selzer, D. Cahen, *Adv. Mater.* **2001**, *13*, 508.
[65] H. Asanuma, E. M. Bishop, H.-Z. Yu, *Electrochim. Acta* **2007**, *52*, 2913.
[66] H. Ishii, H. Sugiyama, E. Ito, K. Seki, *Adv. Mater.* **1999**, *11*, 605.
[67] X. Crispin, V. Geskin, A. Crispin, J. Cornil, R. Lazzaroni, W. R. Salaneck, J.-L. Bredas, *J. Am. Chem. Soc.* **2002**, *124*, 8131.
[68] H. Haick, J. Ghabboun, D. Cahen, *Appl. Phys. Lett.* **2005**, *86*, 042113/1.
[69] H. Haick, J. Ghabboun, O. Niitsoo, H. Cohen, D. Cahen, A. Vilan, J. Hwang, A. Wan, F. Amy, A. Kahn, *J. Phys. Chem. B* **2005**, *109*, 9622.
[70] H. Haick, M. Ambrico, J. Ghabboun, T. Ligonzo, D. Cahen, *Phys. Chem. Chem. Phys.* **2004**, *6*, 4538.
[71] S. Kobayashi, T. Nishikawa, T. Takenobu, S. Mori, T. Shimoda, T. Mitani, H. Shimotani, N. Yoshimoto, S. Ogawa, Y. Iwasa, *Nat. Mater.* **2004**, *3*, 317.
[72] See, e.g., A. Ulman, *An Introduction to Ultrathin Organic Films*, Academic, San Diego **1991**.
[73] A quantitative analysis would require that Equations 3 and 4 be written for each dipole separately. The electric field and dipole become position-dependent and a set of coupled equations need to be solved self-consistently. Such analysis is not pursued here.
[74] A. Vilan, J. Ghabboun, D. Cahen, *J. Phys. Chem. B* **2003**, *107*, 6360.
[75] H. Haick, J. P. Pelz, T. Ligonzo, M. Ambrico, D. Cahen, W. Cai, C. Marginean, C. Tivarus, R. T. Tung, *Phys. Status Solidi A* **2006**, *203*, 3438.
[76] Junctions modified by a *discontinuous* layer of *molecular* dipoles and with an evaporated metal contact, such as the Au/(CH_3-terminated dicarboxylic acid)/n-GaAs one discussed here, produce two main types of contacts: (a) direct metal-semiconductor contacts in the pinhole domains, and (b) metal-molecule-semiconductor contacts.
[77] See, e.g., A. Salomon, D. Cahen, S. Lindsay, J. Tomfohr, V. B. Engelkes, C. D. Frisbie, *Adv. Mater.* **2003**, *15*, 1881.
[78] R. C. Rossi, M. X. Tan, N. S. Lewis, *Appl. Phys. Lett.* **2000**, *77*, 2698.
[79] R. C. Rossi, N. S. Lewis, *J. Phys. Chem. B* **2001**, *105*, 12303.
[80] The term "pinch-off" describes the modulation of electric potential profiles under the low barrier height interface regions, as a result of nm-scale spatial inhomogeneities in the barrier height of the metal/semiconductor contacts.
[81] a) R. T. Tung, *Phys. Rev. B* **1992**, *45*, 13509. b) R. T. Tung, *Mater. Sci. Eng. R.* **2001***, 35, 1.*
[82] P. Bergveld, *Sens. Actuators B* **2003**, *88*, 1.
[83] M. J. Schöning, *Sensors* **2005**, *5*, 126.
[84] K. J. Albert, N. S. Lewis, C. L. Schauer, G. A. Sotzing,, S. E. Stitzel, T. P. Vaid, D. R. Walt, *Chem. Rev.* **2000**, *100*, 2595.
[85] L. Chai, D. Cahen, *Mater. Sci. Eng. C* **2002**, *19*, 339.
[86] D. G. Wu, D. Cahen, P. Graf, R. Naaman, A. Nitzan, D. Shvarts, *Chem. Eur. J.* **2001**, *7*, 1743.
[87] M. Rei Vilar, J. El-Beghdadi, F. Debontridder, R. Naaman, A. Arbel, A. M. Ferraria, A. M. Botelho Do Rego, *Mater. Sci. Eng. C* **2006**, *26*, 253.
[88] J. Song, W. Lu, *Appl. Phys. Lett.* **2006**, 89, 223503.
[89] Y. Rudich, I. Benjamin, R. Naaman, E. Thomas, S. Trakhtenberg, R. Ussyshkin, *J. Phys. Chem. A* **2000**, *104*, 5238.
[90] R. Hoffman, *Solids and Surfaces: A Chemist's View of Bonding in Extended Structures*, VCH, New York **1988**.
[91] See, e.g., A. V. Oppenheim, A. S. Willsky, *Signals and Systems,* Prentice-Hall, London **1983**.
[92] J. Hahm, C. M. Lieber, *Nano Lett.* **2004**, *4*, 51.
[93] F. Patolsky, G. F. Zheng, O. Hayden, M. Lakadamyali, X. W. Zhuang, C. M. Lieber, *Proc. Natl. Acad. Sci. USA* **2004**, *101*, 14017.
[94] Z. Li, Y. Chen, X. Li, T. I. Kamins, K. Nauka, R. S. Williams, *Nano Lett.* **2004**, *4*, 245.
[95] M. Curreli, C. Li, Y. Sun, B. Lei, M. A. Gundersen, M. E. Thompson, C. Zhou, *J. Am. Chem. Soc.* **2005**, *127*, 6922.
[96] A. Star, J.-C. P. Gabriel, K. Bradley, G. Grüner, *Nano Lett.* **2003**, *3*, 459.
[97] A. Star, E. Tu, J. Niemann, J.-C. P. Gabriel, C. S. Joiner, C. Valcke, *Proc. Natl. Acad. Sci. USA* **2006**, *103*, 921.
[98] R. J. Chen, S. Bangsaruntip, K. A. Drouvalakis, N. Wong Shi Kam, M. Shim, Y. Li, W. Kim, P. J. Utz, H. Dai, *Proc. Natl. Acad. Sci. USA* **2003**, *100*, 4984.
[99] The above discussion referred only to dipoles adsorbed on the *sides* of the nano-wire or nano-tube. Dipoles at the edge, i.e., between the nano-tube or nano-wire and, e.g., a metal contact are not considered here. Note, however, that because of the reduced dimensionality at such junctions their behavior is different from that of ordinary Schottky barriers. See, e.g., a) F. Leonard, J. Tersoff, *Phys. Rev. Lett.* **2000**, *84*, 4693. b) S. Heinze, M. Radosavljevic, J. Tersoff, P. Avouris, *Phys. Rev. B* **2003**, *68*, 235418.
[100] a) W. Kohn, *Phys. Rev. Lett.* **1996**, *76*, 3168. b) E. Prodan, W. Kohn, *Proc. Natl. Acad. Sci. USA* **2005**, *102*, 11635.
[101] V. S. L'vov, R. Naaman, V. Tiberkevich, Z. Vager, *Chem. Phys. Lett.* **2003**, *381*, 650.

